Molecular Packing and Diffusion in Polyisobutylene

Richard H. Boyd* and P. V. Krishna Pant

Department of Materials Science and Engineering and Department of Chemical Engineering, University of Utah, Salt Lake City, Utah 84112

Received April 11, 1991; Revised Manuscript Received June 28, 1991

ABSTRACT: Polyisobutylene (PIB) is an elastomer that is notable for low rates of diffusion of small molecules. This has been suggested to be due to efficient intermolecular packing as evidenced by relatively low specific volume. In the present work these questions were studied via simulations. Polyethylene (PE), which is chemically isomeric with PIB, was studied as a comparison material. Monte Carlo simulations of bulk PIB were carried out at constant temperature and pressure, and molecular dynamics simulations of methane diffusion in both polymers were made. The MC simulations result in lower specific volumes for PIB compared to PE, as observed experimentally. The more efficient packing in PIB is attributed to the unoccupied volume in the systems being largely at the intermolecular interfaces and thus a molecular surface phenomenon. The thicker cross-sectioned PIB molecules have less surface area per carbon atom. The MD simulations show a slower diffusion rate in PIB. Further simulations at different densities show the diffusion to be very sensitive to small volume changes. For example, diffusion in PIB at the experimental density of polyethylene is calculated to be faster than for PE at this density.

Introduction

Polyisobutylene (PIB) is an interesting polymer from several standpoints. Even though it is sterically hindered with respect to skeletal bond rotations[1] it has a low glass temperature.[2] Thus, although it is capable of crystallization, low crystallization temperatures and sluggish kinetics permit its use as an important elastomer.[3] In comparison with many other common elastomers, it has a markedly low permeability to small-molecule penetrants or diffusants.[4] Elastomeric PIB has a rather high density or low specific volume. For example, PIB is chemically isomeric with polyethylene (PE) but the liquid specific volume at 400 K of the latter is 9% higher.[5,6] It has been conjectured that the permeability characteristics of PIB are related to the low specific volume. In the present work we investigate via Monte Carlo (MC) simulations the details of the molecular packing that lead to low specific volume and by molecular dynamics (MD) simulations the diffusion of small penetrants. PE was employed as a basis for comparison. Packing details in PIB are compared to previous MC simulation results for PE,[7] and companion MD simulations of penetrant diffusion are carried out here for PE as well.

Simulation Details

Potential Functions. In our previous alkane MC simulations,[7,8] in order to reduce computational complexity, the commonly invoked approximation of using a contracted hydrogen or a "united-atom" effective $-CH_2-$ group nonbonded potential was used. We continue to contract the hydrogen atoms and to use united-atom nonbonded potentials. For PIB three group types are present, >C<, $-CH_2-$, and $-CH_3$; see Figure 1. For $-CH_2-$ groups, the previous potential[7,8] was used. For >C<, the Lennard-Jones "6–12" potential was chosen to have the same r_{min} and well-depth, ϵ, as the C···C "exponential-6" potential employed in general in our previous molecular mechanics calculations.[9,10] The latter exp-6 potential is used for all types of attached atoms including when the hydrogens are explicitly included. For $-CH_3$, a new group nonbonded potential was calibrated. It is based on reproduction of the unit cell parameters of crystalline PIB. The unit cell parameters[11] are sensitive to r_{min} and somewhat to ϵ. Methodology previously described[12] was used to find the energy-minimized unit cell parameters for assumed r_{min} and ϵ values. Table I shows results for several choices including the selected ones. We were also influenced in the ϵ choice by a value advocated by Jorgensen et al.[13] and found from optimizing MC simulations of small-molecule liquids against density and heat of vaporization.

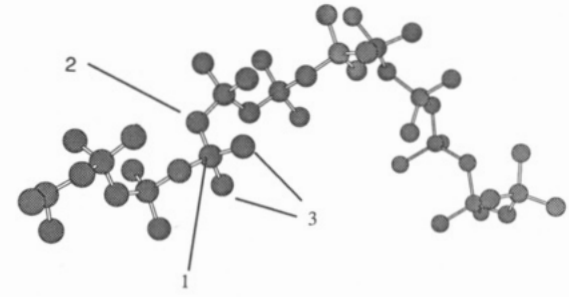

Figure 1. Bead or contracted hydrogen united-atom representation of PIB. There are three types of such beads in PIB, (1) >C<, (2) $-CH_2-$, and (3) $-CH_3$. The chains employed have 24 main-chain carbon atoms and 24 pendent $-CH_3$ beads.

The penetrant studied was methane, and it was also represented as united atoms. The potential used is a slight adaptation of one previously developed.[14] That "n–6" potential, with $n = 11.2$, was altered to keep the same ϵ and r_{min} but n changed to 12.

Table II summarizes all of the nonbonded potentials used for like pairs. The parameters for unlike pairs were determined by taking $A_{12} = (A_{11}A_{22})^{1/2}$ and $B_{12} = (B_{11}B_{22})^{1/2}$ in the formulation $U = AR^{-12} - BR^{-6}$.

It has been previously found in molecular mechanics calculations on PIB that when intramolecular nonbonded interactions are superposed upon a 3-fold intrinsic torsional barrier for the skeletal bonds, the three expected minima are each split into two minima separated by a shallow barrier.[1] In addition, the intramolecular nonbonded interactions cause considerable steric strain that forces open the skeletal valence angle at the $-CH_2-$ group to an exceptionally large value. The hydrogen-contracted group nonbonded potentials do not lend themselves to describing these close-by intramolecular interactions. In the previous PE simulations,[7,8] the four-center intramolecular nonbonded interactions were dispensed with and a single-fold torsional potential was used to establish the gauche trans energy difference. Here both four- and five-center intramolecular interactions were omitted. Only a 3-fold

0024-9297/91/2224-6325$02.50/0

Table I
CH_3 Nonbonded Parameters and Unit Cell of PIB

potential param[a]		calcd unit cell param	
ϵ, kJ/mol	r_{min}, Å	a, Å	b, Å
0.495	4.335	11.48	6.46
0.495	4.55	11.80	6.65
0.711	4.55	11.88	6.69
0.495	4.65	11.97	6.75
0.711	4.65	12.04	6.80
		exptl unit cell[b]	
		11.91	6.88

[a] Well-depth and minimum distance in Lennard-Jones 6–12 potential. [b] From ref 11.

torsional potential was used, as it gave a reasonable representation of the characteristic ratio. The valence angle distortion was introduced via setting the relaxed angle at $-CH_2-$ to 122°.

In the MC calculations the bond angles and lengths were kept fixed but in the MD simulations both were free to vary under the potential functions listed in Table II. The force constants for bending and stretching were previously used[8] and were selected to be realistic representations consistent with spectroscopic force constants. No downward adjustment to accommodate shorter time steps was made.

Monte Carlo Simulations. The isothermal, isobaric MC simulation method used is similar to that previously described for long-chain alkanes employed as models for PE.[7] Reptation is employed as the basic move. In alkanes, a CH_2 bead is clipped from one chain end and attached at the other end at a randomly selected torsional angle. From the energy change, the Metropolis rules[15] are used to accept or reject the move. In addition to the reptational moves, occasionally volume fluctuations under an imposed external pressure are attempted and also evaluated for acceptance from the energy change using the Metropolis criteria.

In the reptational move strategy it is essential that the entity being moved be kept as simple as possible. That is, there must be sufficient space for the clipped group to be inserted that there is a reasonable acceptance rate. In PIP this dictates that individual >C<, $-CH_2-$, or $-CH_3$ groups be transferred. As seen in Figure 2, this leads to four types of end groups and two types of chains (chain 1 vs chain 4 in Figure 2). The chains employed had 24 main-chain beads in order to be directly comparable with the previous PE simulation. Thus, each chain also contained 24 CH_3 pendent groups for a total of 48 beads. A periodic box with 18 such chains was employed. The original starting point for the simulations was a somewhat oversized box (33-Å edge), for the eventual specific volumes to be reached, packed with a regular array of TG helices (the crystal conformation); see Figure 3. As reptations proceed and the isobaric volume fluctuations accumulate, the system becomes disordered and the box size changes until it fluctuates about an eventual equilibrium value (Figure 4). Further runs with different temperatures, for example, were started from disordered systems that were the final points of other runs.

Since PIB has four groups or beads per monomer unit compared to two for PE, it requires twice as many reptational transfers to accomplish the same main-chain movement in the former as in the latter. Since the net reptational motion is diffusive in character and thus proportional to the number of moves, N, as $N^{1/2}$, it is expected that ~4 times as many moves would be required to achieve the same progress in PIB as in PE. In fact it was observed that equilibration was considerably slower in PIB. More attempts were required, and equilibration was limited to temperatures of 400 K and above.

Molecular Dynamics and Diffusion. MD runs were carried out on the PIB systems described above and also on PE systems like those previously described.[7] The latter consist of periodic boxes of 32 chains each with 24 methylene units. The MD calculations were carried out on both N, V, E and N, V, T ensembles. The N, V, E calculations were used to establish the time step necessary to ensure conservation of energy. A value of 0.5 fs was adopted. This is a rather small value, but the bond stretching and bending force constants in the potential functions were taken to be realistic values and were not weakened in order to lengthen the time step. In the actual diffusion calculations the N, V, T ensemble was employed. The constant-temperature method used was that of Berendsen et al.[16] The integration of Newton's equations was carried out using the "velocity Verlet" method.[17] The nonbonded function cut-off radius was 9 Å.

The diffusion of methane in both PIB and PE was studied. Methane was selected as a small-molecule penetrant because among such molecules as O_2, N_2, CO_2, and CH_4 commonly studied in this role it is closest to actually having the spherical symmetry implied by representation of the potentials by contraction to a single force center. In addition, the like pair potential is well calibrated. It was found that when even only a few molecules were injected, significant correlations between the penetrant molecules were found. Thus, to keep interpretation simple, only one penetrant molecule per periodic box was employed. Even with only one particle, sufficiently good statistics could be obtained over reasonably short trajectories that reliable diffusion coefficients could be determined. The self-diffusion coefficients, D_2, for the penetrant, labeled as 2, were obtained from the slopes of plots of the mean-square particle displacement vs time, t, using the standard relation[18]

$$\lim_{t \to \infty} \langle R^2 \rangle / t = 6D_2 \tag{1}$$

The mutual diffusion coefficient is dependent on the diffusion of the center of mass of the penetrants. Under the conditions here of only one penetrant molecule, no correlations exist between the penetrant trajectories and the mutual diffusion coefficient is the same as the self-diffusion coefficient apart from a factor dependent on the equilibrium structure that is usually approximated as unity.[18] Trohalaki et al.[19] in their MD study of CO_2 diffusion in PE also found strong penetrant motion correlations. Their mutual diffusion coefficients for four penetrant molecules were several times larger than the self-diffusion coefficients.

In determining $\langle R^2 \rangle$, the technique of regarding, in principle, each point along a raw, unsmoothed trajectory as the starting point of a new trajectory[18] was employed. $\langle R^2 \rangle$ at time t may thus be determined by averaging over all possible time origins in the raw trajectory. For this averaging to be reliable at the longest time of interest, a fairly large number of independent trajectories of this length need to be available. The complete trajectory, from start to finish of a run, was therefore several times longer than the longest intermediate ones used to compute $\langle R^2 \rangle$ values to plot against t. In practice, every tenth time step was used for fixing the trajectory starting points.

All of the calculations of both MC and MD were carried out on an IBM 3090 600VS computer using vectorized FORTRAN codes. The computation time for a 4M attempt MC run on PIB was ~7800 CPU seconds. For

Table II
Potential Functions[a]

function	constants	
harmonic C–C bond stretch = $(1/2)k_R(R - R_0)^2$	k_R = 2650	R_0 = 1.54
harmonic bond bending = $(1/2)k_\theta(\theta - \theta_0)^2$		
$-CH_2-$ (PIB)	k_θ = 482	θ_0 = 122.0°
$-CH_2-$ (PE, MD[b])	k_θ = 482	θ_0 = 111.6°
$-CH_2-$ (PE, MC)		θ_0 = 109.47°
$>C<$	k_θ = 482	θ_0 = 109.47°
torsional potential = $(1/2)V_3(1 + \cos 3\phi)$	V_3 = 13.4	
nonbonded potentials, Lennard-Jones 6–12[c]		
$-CH_2-$	ϵ = 0.495	R_{min} = 4.335 σ = 3.86
$>C<$	ϵ = 0.397	R_{min} = 3.872 σ = 3.45
$-CH_3$	ϵ = 0.732	R_{min} = 4.65 σ = 4.14
CH_4	ϵ = 1.18	R_{min} = 4.27 σ = 3.80

[a] Energies are in kJ/mol, distances in Å, and angles in radians (shown above in degrees). [b] The $-CH_2-$ valence angle was taken as tetrahedral in the MC simulations of ref 7 but changed here in the MD simulations to a slightly larger and more realistic value. [c] ϵ is the well-depth, R_{min} is the distance of the minimum, and σ is the distance where potential crosses zero.

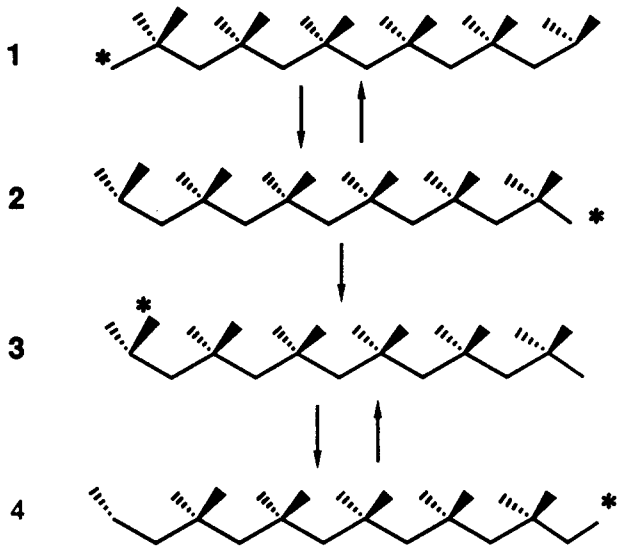

Figure 2. Reptation a bead at a time in PIB. Moving the starred bead in chain 1 creates chain 2 and vice versa. Moving the starred bead in chain 3 (identical to chain 2) creates chain 4 and vice versa.

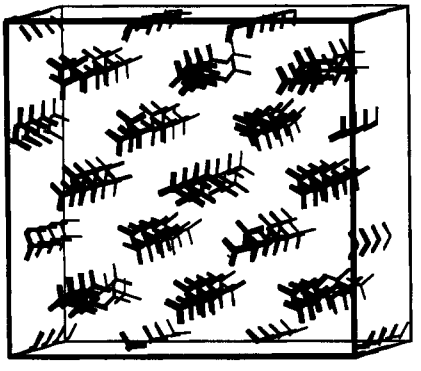

Figure 3. Initial system at the start of PIB MC simulation. Periodic box, of edge length 33 Å, packed with 18 chains as a regular array of TG helices.

a 50-ps MD run (smoothed to 20 ps), the computation time was ~32 000 CPU seconds.

Packing in PIB and PE. Volume versus temperature results from the MC simulations for PIB and PE are displayed in Figure 5. Also shown are experimental results[5,6] for high molecular weight PE and PIB. The simulation results on the C_{24} alkane are somewhat higher (~5%) than experiment for PE. Since experimentally the specific volume of C_{24} is even higher, ~7%, than high molecular weight PE, this has been previously attributed

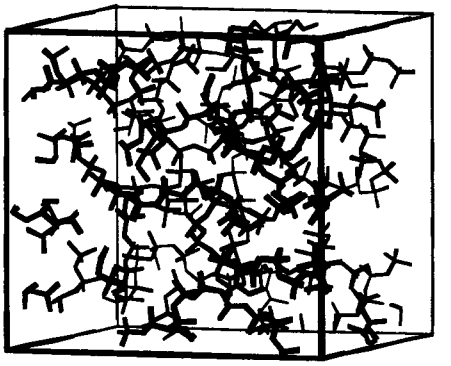

Figure 4. Snapshot of system of Figure 3 after reptation, volume fluctuation MC equilibration. T = 500 K, P = 1 atm.

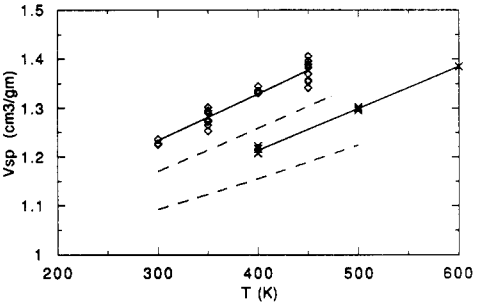

Figure 5. Specific volume vs temperature (at 1 atm) from MC simulations for C_{48} PIB (crosses) and C_{24}PE (open diamonds, results from ref 7). The upper dashed curve is the experimental volume for high molecular weight PE (from ref 6) and the lower one is for high molecular weight PIB (from ref 5).

to a finite molecular size effect.[7] There is no appropriate oligomer experimental density data for PIB. However, the offset of the simulations from high molecular weight experimental data is similar to that for PE, an apparently reasonable result as the main-chain carbon atom lengths are the same in both simulations. It is gratifying to note that the simulations do in fact result in calculated specific volumes that are higher for PE than for PIB. The ratio of the calculated oligomer volumes for PE vs PIB is about the same (~9% higher for PE at 400 K) as found experimentally in the high molecular weight case. With the more efficient packing in PIB demonstrated by simulation it is appropriate to investigate the reasons for this. This is taken up below.

It is useful to divide the volume in the systems into two categories, as occupied or unoccupied. This is discussed more fully in the context of diffusion below. From that analysis, on the basis of assigning the groups spherical

Figure 6. Space-filling views of PIB (lower) and PE (upper) chains generated by assigning van der Waals radii = $\sigma/2$ of Table II to the groups.

diameters (Figure 6) equal to the repulsion diameter, σ, the unoccupied fraction in PE is 0.37 and in PIB is 0.29 (both at 300 K). From the specific volumes of the systems used to compute these fractions, it follows that the occupied volume for PE is 0.74 cm^3/g and for PIB is 0.77 cm^3/g. The unoccupied volumes are 0.43 and 0.32 cm^3/g, respectively. Thus, in this picture, PE is slightly more compact than PIB in terms of occupied volume but is less well packed in terms of unoccupied volume. Thus it is appropriate to look at the intermolecular packing features.

The most prominent structural difference between PIB and PE concerns their respective cross-sectional areas. PIB having the same atomic composition in one monomeric unit as two units in PE is thus shortened by a factor of 2 in main-chain atoms for the same total atom count. This is accompanied by an increase in the effective cross-sectional area. In Figure 7, the radial distribution functions (RDF's) for PIB and PE from MC simulation are displayed. In Figure 8, the intermolecular contributions to the radial distribution functions are compared. In Figure 9, a main-chain group site intermolecular RDF, based on the distance of either a $-CH_2$ or a >C< group to any group on another molecule, is displayed and compared with the same PE intermolecular RDF as shown in Figure 8. In Figure 10, a pendent $-CH_3$ group site intermolecular radial distribution function, based on the distance from any $-CH_3$ group to any group on another molecule, is shown along with the PE intermolecular RDF. The cross-sectional area differences between PIB and PE are readily apparent in Figures 7–10. In the intermolecular RDF, Figure 8, PE shows a distinct maximum at ~5.5 Å, which presumably can be interpreted as an average interchain distance. In PIB, the intermolecular RDF (Figure 8) and the site intermolecular RDF's (Figures 9 and 10) rise to about 7 Å, a result of the greater interchain spacing, and there appears to be no distinct maximum. The lack of a well-developed maximum presumably reflects not only the thicker PIB chains but also the skewing effect about the maximum, evident for PE in Figure 8, of increased aperture of the farther side of a neighboring chain relative to the near side.

Roughly viewed, the packing in PE can be interpreted very locally as packed tubes or cylinders of diameter equal

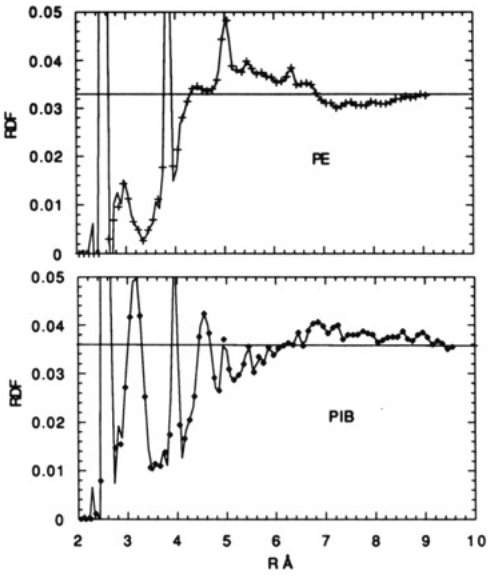

Figure 7. Radial distribution function from MC simulation, expressed as the number density (particles/Å^3), for PIB (lower plot, filled diamonds) and PE (upper plot, crosses), 400 K. Same data are used in Figures 8–10. The average number density is indicated by horizontal lines.

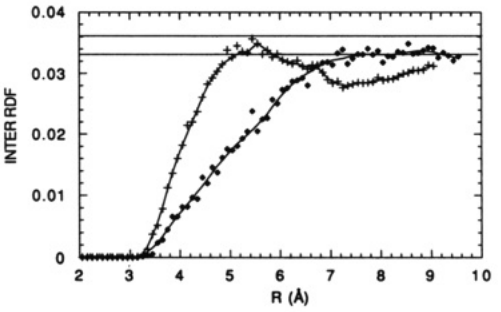

Figure 8. Intermolecular radial distribution function, based on the distance from any group to any group on another molecule, from MC simulation for PIB (filled diamonds) compared with PE (crosses). The average total number density is indicated by horizontal lines.

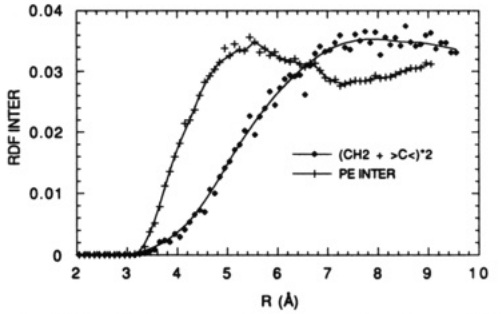

Figure 9. Main-chain atom site intermolecular radial distribution function for PIB (filled diamonds), based on distance from $-CH_2-$ or >C< groups to any other group on another molecule. It is normalized for comparison with the PE intermolecular radial distribution function (crosses) by multiplying the actual number density by 2.

to the RDF maximum and height based on the 1–3 spacing in C(1)–C(2)–C(3). That is, for close-packed cylinders, the volume per $-CH_2-$ is $3^{1/2}d^2h/2$ where d is the cylinder diameter or intercylinder spacing and h the height per $-CH_2-$. For the specific volume of 1.33 cm^3/g for the PE system in Figure 8 and h = 1.257 Å this gives a intermolecular spacing equal to 5.33 Å. This compares fairly well with the 5.5-Å spacing observed in Figure 8. A similar calculation can be carried out for PIB. The average 1–3

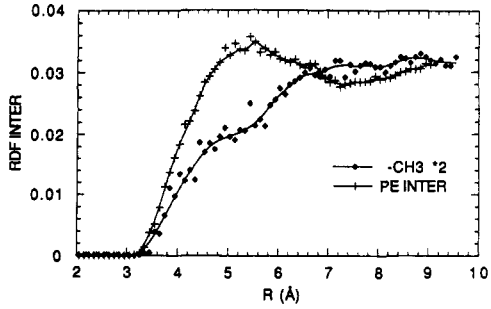

Figure 10. Pendent methyl group site intermolecular radial distribution function for PIB (filled diamonds), based on the distance from $-CH_3$ groups to any other group on another molecule. It is normalized for comparison with the PE intermolecular radial distribution function (crosses) by multiplying the actual number density by 2.

spacing in the two types of C(1)–C(2)–C(3) sequences gives a per bond height of 1.30 Å. This leads, from the specific volume of 1.21 cm^3/g for PIB in Figure 8, to an interchain spacing of 7.1 Å. Since no defined maximum is observed in the RDF's, it is not possible to make a good comparison with the simulation results. However, if the interchain spacing has a value that is ~0.2 Å higher than the value from the packed cylinder calculation, as in PE, then the RDF's, Figure 9 for example, would appear to be at least consistent with this. That is, it is well into the leveled-out region beyond 7 Å.

Thus, although the above picture is very approximate and should not be pushed too far, it appears that it is useful to think of the density as being determined by the local packing of cylinders. This leads to a simple interpretation of the more efficient packing in PIB. If, in the packed-cylinder view, the cylinders were internally of uniform density and of the same density in the two polymers, then the packing efficiency would be the same. That is, for close-packed cylinders the fractional occupied cross-sectional area is independent of cylinder radius. However, a better picture is to view the cylinders as having a poorly packed region about their surfaces. The unoccupied volume appearing in the occupied versus unoccupied analysis above occurs obviously between the chains and is to be associated with the chain surfaces. Therefore, it is useful to think of the cylinders as having a dense core and a poorly packed surface or interfacial layer between them. Then it is also useful to suppose that the poorly packed surface layer is of similar thickness in both polymers. The $-CH_3$ site RDF for PIB in Figure 10 rises steeply initially, the same region as the RDF for PE indicating similar chain–chain contact distances in the two polymers. In the dense core-fuzzy surface picture, there is a packing efficiency advantage for the higher cross-sectional area, thicker PIB chains. An unpacked interchain standoff gap of ~1 Å between contacting chains in addition to the dense-packed core in both polymers would explain the lower specific volume of PIB.

It is of interest to comment on the characteristic ratio from the simulations for PIB. It is appropriate to observe that, for the chain lengths used in the simulations for both PE and PIB, the characteristic ratios are somewhat chain length dependent and have not yet reached the asymptotic long-chain values.[20] This effect must be considered in making comparison with experimental values. At 400 K, a value of the mean-square end-to-end distance of $\langle r^2 \rangle$ = 280 $Å^2$ was found for PIB. For n = 23 bonds and l = 1.54 Å this leads to C_n = 5.1. This compares to previous simulation results for PE from which $\langle r^2 \rangle$ = 300 $Å^2$ at the same temperature and C_n = 5.5 Å.[7] It was previously shown that the latter value is in good agreement with an RIS calculation for this chain length. The RIS parameters are also consistent with the characteristic ratio for high molecular weight PE. The experimental value for PIB is 6.6 at 300 K.[20] The experimental temperature coefficient for PIB is believed to be small,[20] and the value at 400 K is ~6.5. This is to be compared to 6.7 (at 400 K) for PE.[21] Thus the slightly smaller C_n value compared to PE found by simulation for PIB appears to be consistent with experiment for PIB of this chain length.

Table III
Calculated Cohesive Energy and Solubility Parameter of PIB[a]

T, K	V specific, cm^3/g	E cohesive,[b] cal/mol	δ, solubility param, $(cal/cm^3)^{1/2}$	δ exptl, $(cal/cm^3)^{1/2}$
500	1.30	820	6.7	
400	1.21	912	7.3	
298			7.9 extrapolated	7.7–8.1[c]

[a] Values from the simulations on a C_{48} oligomer. [b] The intermolecular nonbonded energy per mole of carbon atoms. [c] Range of tabulated values from various sources in ref 2.

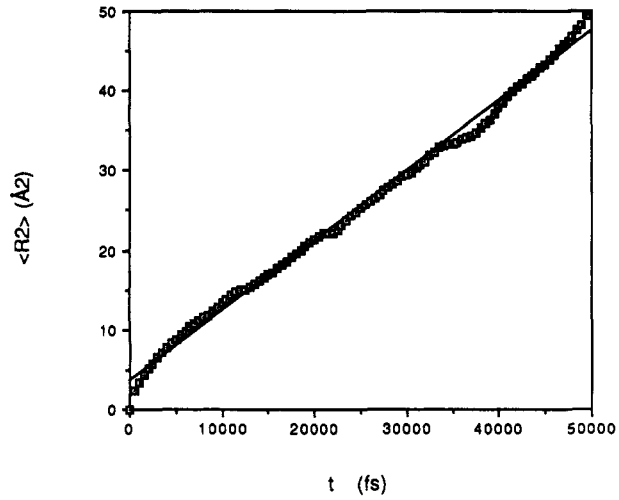

Figure 11. Averaged R^2 for diffusing methane molecule versus time in PE at 300 K.

From the intermolecular nonbonded energy and the specific volumes, the simulations can be used to compute the cohesive energy density and solubility parameters of the polymers. We have already shown that the cohesive energies for PE from simulation are in good agreement with experiment.[8] For PIB, results are listed in Table III. The derived solubility parameter at 25 °C is in good agreement with tabulated values.

Diffusion in PIB and PE. In the MC simulations constant-pressure conditions were employed and the volume follows from the calculations. In the MD studies, however, constant-volume conditions were imposed. In this circumstance, the volume has to be chosen and we elected to use the experimental volumes for the high molecular weight polymers (Figure 5).

A R^2 versus t curve, smoothed as described above under simulation details, for a long run for methane in PE at 300 K is shown in Figure 11. Except for an initial faster portion, it may be seen that the best fit line drawn is representative of the data at relatively short times as well as long ones. Thus it is believed that reliable diffusion coefficients can be determined from much shorter runs than the one displayed here, and in fact the averaged runs used for most of the work were 20 ps in extent (50–100-ps longest trajectory). It is to be emphasized that curves such as this

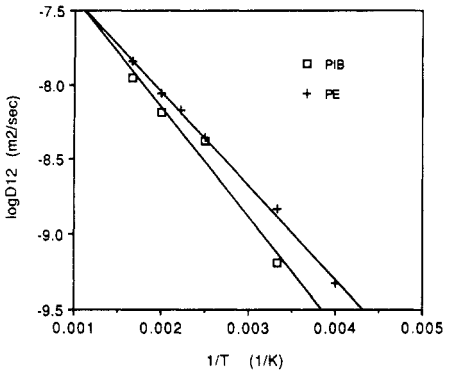

Figure 12. Self-diffusion coefficients of methane in PE and PIB from MD simulations plotted in Arrhenius form. The activation energy in PE is 11.9 kJ/mol and 14.0 kJ/mol in PIB.

represent the average progress as the result of diffusion. The actual raw trajectories show local excursions considerably greater in extent than the smoothed $\langle R^2 \rangle$ values. Over a very short time interval a raw trajectory shows a relatively fast motion that is interrupted by collision-like events. Thus even the smoothed $\langle R^2 \rangle$ curves at very short times show a faster behavior, more like $\langle R^2 \rangle$ proportional to t^2. This results in an apparent positive intercept in the $\langle R^2 \rangle$ vs t curves.

Diffusion results for methane in both polymers at several temperatures are shown in Figure 12 in the form of Arrhenius plots. Each point in the figure is derived from the slope of a $\langle R^2 \rangle$ vs t plot. The regression coefficients, r^2, of the least-square fits to the latter plots were 0.97 or higher with the exception of the 250 K run for PE where it was 0.933. It is apparent that the simulations do in fact show that the diffusion is slower in PIB than PE. It is not possible to make precise comparisons with experiment for the absolute values. However, it is obvious that the calculated results are considerably too high. Data for methane diffusion in PE is clouded by the presence of crystallinity. In low-density PE, of degree of crystallinity of ~40%, the measured value at 25 °C is 0.19×10^{-10} m^2/s.[4] A linear volume fraction correction would indicate a value of $\sim 0.3 \times 10^{-10}$ m^2/s for the amorphous fraction. This compares with the calculated value here (Figure 12) of 12×10^{-10} m^2/s. For PIB no reported experimental values were found for methane. However, values at 25 °C for small penetrants such as CO_2, N_2, and O_2 are in the range $0.06 \pm 0.2 \times 10^{-10}$ m^2/s.[4] These are to be compared with 6.2×10^{-10} m^2/s from simulation. The activation energies experimentally are in the range of 50 kJ/mol, and the calculated ones are 12–14 kJ/mol (Figure 12). The simulation by Trohalaki et al.[19,21] also found much higher results for the diffusion coefficients and lower values for the activation energies than experimental for CO_2 in PE and so did Takeuchi and Okazaki[22] for O_2 in PE. In fact, the self-diffusion coefficients and activation energies found by Trohalaki et al.[19] are very comparable to our results. Their mutual diffusion coefficients, obtained for systems with several penetrant molecules, were substantially higher, more than an order of magnitude at 300 K, than the calculated self-diffusion coefficients. Thus it is apparent that the MD simulations give results that are considerably too high. The reasons for this are not known. Takeuchi[23] investigated the effect of the rather small degrees of polymerization of the molecules employed and carried out a simulation on an infinite molecular weight polymer. It was concluded that this effect was rather small. In our work we have used realistic stretching and bending force constants and a very small time step for integration. This would indicate that internal vibration amplitudes

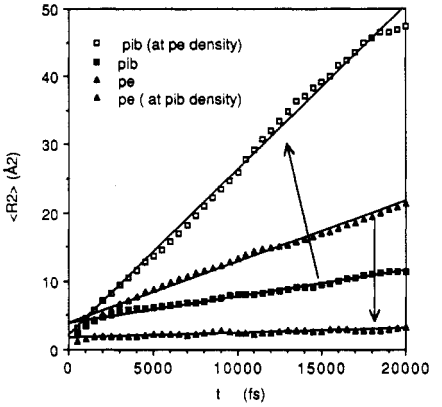

Figure 13. Averaged R^2 versus time for methane diffusing in PE (filled triangles) and PIB (filled squares) at their respective densities and for PE at the density of PIB (open triangles) and PIB at the density of PE (open squares) at 300 K. Arrows indicate the effect of density change for each of the two polymers. All densities are experimental ones for high molecular weight polymers.

are not a major issue per se. It may well be that united-atom group nonbonded potentials, even though calibrated to give good packing energies and volumes, are not detailed enough to represent the local barriers to penetrant motion accurately.

Although the absolute values of the diffusion coefficients are not of high accuracy, the relative values between the polymers are better and it is appropriate to make some further exploration of the reasons for the slower diffusion in PIB relative to PE. As mentioned above, it has been speculated that this is related to the lower specific volume of PIB. Thus simulations were made of the effect of density on diffusion. Specifically, runs were made on PIB constrained to the experimental specific volume of PE and vice versa. These results are displayed in Figure 13. It may be seen that indeed the rather small volume alterations have a dramatic effect on the rates. PE at the specific volume of PIB now has the slowest rate of diffusion. PIB at PE specific volume has a higher diffusion coefficient than PE at its own normal specific volume.

It is interesting to analyze the above effects in terms of free volume. To that end, the volume of the simulated systems was assigned as occupied or unoccupied based on van der Waals spheres of the repulsive diameter, σ, as given in Table II. In addition, the unoccupied volume was analyzed, as previously described,[8] as to how much of it is available to a probe sphere of a given radius. The results of this analysis are given in Figure 14. Looking first at PE and PIB at their own specific volumes in Figure 14, it may be seen that PIB does have a lower *total* fractional free volume; i.e., the value for $R = 0$, in agreement with the lower diffusion rate for the latter. It may be seen, however, that the curves versus R for these two cross over at 0.4–0.5 Å and the free volume situation is reversed at larger R values. PIB at PE density of course has the same volume as PE but it is also very nearly total iso free volume as well ($R = 0$ intercept in Figure 14). Diffusion in PIB at PE density is found from simulation to be considerably faster than in PE however (Figure 13). The curves versus R do diverge with an increase in R and in the right direction. At $R > \sim 0.2$ Å, PIB at PE density has the highest fractional free volume of the four cases in agreement with the diffusion results. Diffusion in PE at PIB density is found to have a lower diffusion rate than PIB (Figure 13) but the total fractional free volume of the latter is less. The curves versus R cross over, however, at a relatively low R value and at $R > \sim 0.3$ Å, the fractional

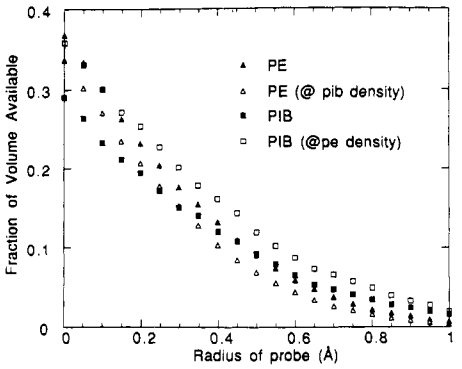

Figure 14. Fractional system volume available to a probe sphere of radius R versus the radius of the sphere. Results for PIB and PE and for PIB at the specific volume of PE and vice versa. Specific volumes are the experimental ones used in the MD diffusion simulations at 300 K.

volume available is less in PE at PIB density in agreement with the diffusion results. All of the above conclusions also prevail when unoccupied absolute volume rather than fractional volume is considered.

Thus overall it would appear proper to conclude that diffusion is extremely sensitive to polymer density and that the more efficient packing in PIB is responsible for low diffusion rates in it. However, there does not appear to be a simple free volume criteria for sorting out the finer details.[24]

Acknowledgment. We are grateful to the Exxon Chemical Co. for financial support of this work and especially to Mr. J. V. Fusco and Dr. G. Ver Strate for their interest and helpful comments. We are also greatly indebted to the Utah Supercomputing Institute where the computations were performed. We thank Dr. Wen-Bin Liau for carrying out the unit cell calculations for PIB.

References and Notes

(1) Boyd, R. H.; Breitling, S. M. *Macromolecules* **1972**, *5*, 1.
(2) Brandrup, J.; Immergut, E. H. *Polymer Handbook*, 3rd ed.; Wiley-Interscience: New York, 1989.
(3) Mark, H. F.; Gaylord, N. G.; Bikales, N. M. *Encyclopedia of Polymer Science and Technology*; Wiley-Interscience: New York, 1965; Vol. 2.
(4) Crank, J.; Park, G. *Diffusion in Polymers*; Academic Press: New York, 1968.
(5) Eichinger, B. E.; Flory, P. J. *Macromolecules* **1968**, *1*, 285.
(6) Beret, S.; Prausnitz, J. M. *Macromolecules* **1975**, *8*, 536.
(7) Boyd, R. H. *Macromolecules* **1989**, *22*, 2477.
(8) Boyd, R. H.; Pant, P. V. K. *Macromolecules* **1991**, *24*, 4078.
(9) Chang, S.; McNally, D.; Shary-Tehrany, S.; Hickey, M. J.; Boyd, R. H. *J. Am. Chem. Soc.* **1970**, *92*, 3109.
(10) Sorensen, R. A.; Liau, W. B.; Kesner, L.; Boyd, R. H. *Macromolecules* **1988**, *21*, 200.
(11) Tanaka, T.; Chatani, Y.; Tadokoro, H. *J. Polym. Sci., Polym. Phys. Ed.* **1974**, *12*, 515.
(12) Sorensen, R. A.; Liau, W. B.; Boyd, R. H. *Macromolecules* **1988**, *21*, 194.
(13) Jorgensen, W. L.; Madura, J. D.; Swenson, C. J. *J. Am. Chem. Soc.* **1984**, *106*, 6638.
(14) Breitling, S. M.; Jones, A. D.; Boyd, R. H. *J. Chem. Phys.* **1971**, *54*, 3959.
(15) Metropolis, N.; Rosenbluth, A. N.; Rosenbluth, M. N.; Teller, A. H.; Teller, E. J. *J. Chem. Phys.* **1953**, *21*, 1087.
(16) Berendsen, H. J. C.; Postma, J. P. M.; vanGunsteren, W. F.; DiNola, A.; Haak, J. R. *J. Chem. Phys.* **1984**, *81*, 3684.
(17) Swope, W. C.; Andersen, H. C.; Berens, P. H.; Wilson, K. R. *J. Chem. Phys.* **1982**, *76*, 637.
(18) Jolly, D. L.; Bearman, R. J. *Mol. Phys.* **1980**, *41*, 137.
(19) Trohalaki, S.; Rigby, D.; Kloczkowski, A.; Mark, J. E.; Roe, R. J. *Polym. Prepr. (Am. Chem. Soc., Div. Polym. Chem.)* **1989**, *30* (2), 23.
(20) From a tabulation in: Flory, P. J. *Statistical Mechanics of Chain Molecules*; Interscience: New York, 1969.
(21) Trohalaki, S.; Kloczkowski, A.; Mark, J. E.; Rigby, D.; Roe, R. J. In "*Computer Simulation of Polymers*"; Roe, R. J., Ed.; Prentice-Hall: Englewood Cliffs, NJ, 1991; p 220.
(22) Takeuchi, H.; Okazaki, K. *J. Chem. Phys.* **1990**, *92*, 5643.
(23) Takeuchi, H. *J. Chem. Phys.* **1990**, *93*, 4490.
(24) For a discussion of diffusion and its relation to another definition of free volume, see: Takeuchi, H.; Roe, R. J.; Mark, J. E. *J. Chem. Phys.* **1990**, *93*, 9042.